Crystal Structure of Cu-Zn-Al Martensite

M. Zolliker, W. Bührer, Labor für Neutronenstreuung,
ETH Zürich; R. Gotthardt, IGA, EPF Lausanne;
J. v. Humbeeck, University Leuven

Choice of Monoclinic Unit Cell

M18R is nearly a close-packed structure. The common way to describe the stacking sequence is the A B C-notation:

A B' C B' C A' C A' B A' B C' B C' A C' A B'

This description implies a unit cell with a height of 18 planes. But the true crystallographic unit cell is only 6 planes high and face centered on one side. It becomes visible with the "h-k"- or the with the "△-▽"- notation (1):

h k' h h' k h' h k' h h' k h' h k' h h' k h'

△ △ ▽ △ △ ▽ △ △ ▽ △ △ ▽ △ △ ▽ △ △ ▽

<-- unit cell -->

Whereby:
"h" means near hexagonal-close-packed neighbourhood (A B A)
"k" means near cubic-close-packed neighbourhood (A B C)
"▽" means right shift of upper plane
"△" means left shift of upper plane

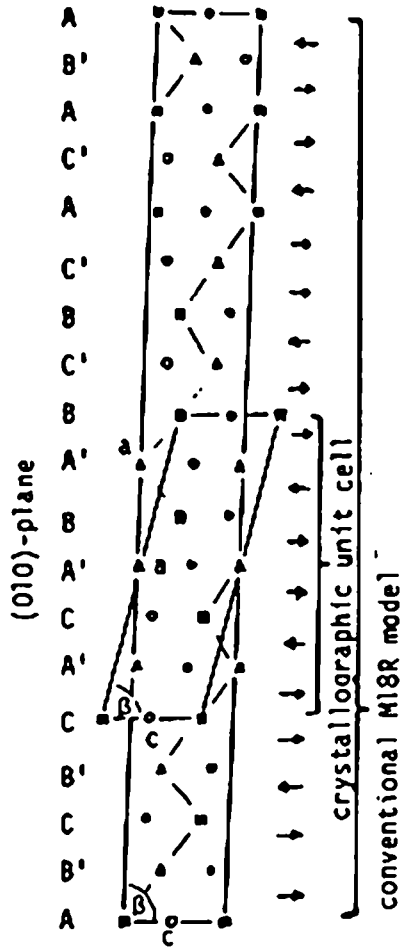

Conventional M18R model	Crystallographic unit cell
space group P m	space group C/2 m
a = 38.3 Å	a = 13.2 Å
b = 5.34 Å	b = 5.34 Å
c = 4.42 Å	c = 4.42 Å
β = 88.5	β = 75.6

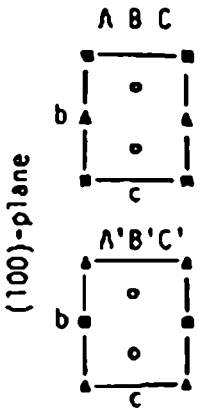

occupation numbers for $Cu_{.65}Zn_{.20}Al_{.15}$ (2)

o	Cu 1.0		
■	Cu 0.6	Zn 0.4	
▲		Zn 0.4	Al 0.6

Fig. 1: conventional M18R model and crystallographic unit cell

This three times smaller unit cell has more symmetry elements than in the conventional M18R model. The irreducible asymetric unit is even 12 times smaller taking into account the face centering and the symmetry centre.

Neutron Powder Diffraction measurements

Elastic neutron diffraction measurements have been performed on powders. The experimental data were compared with the model calculations. The measured peak positions correspond nearly to the expected values, i.e. the lattice parameters are correct. However, a refinement of the atomic positions, the sublattice occupations and the Debye-Waller factors does not converge to a satisfactory agreement of the observed intensities and the computed structure factors. A detailed study of the difference between measured and calculated neutron intensities shows two kinds of faults: Some peak widths (marked by arrows, Fig. 2) and some peak positions (marked by asterisk) do not agree. To improve the model, it is required to take stacking faults into consideration.

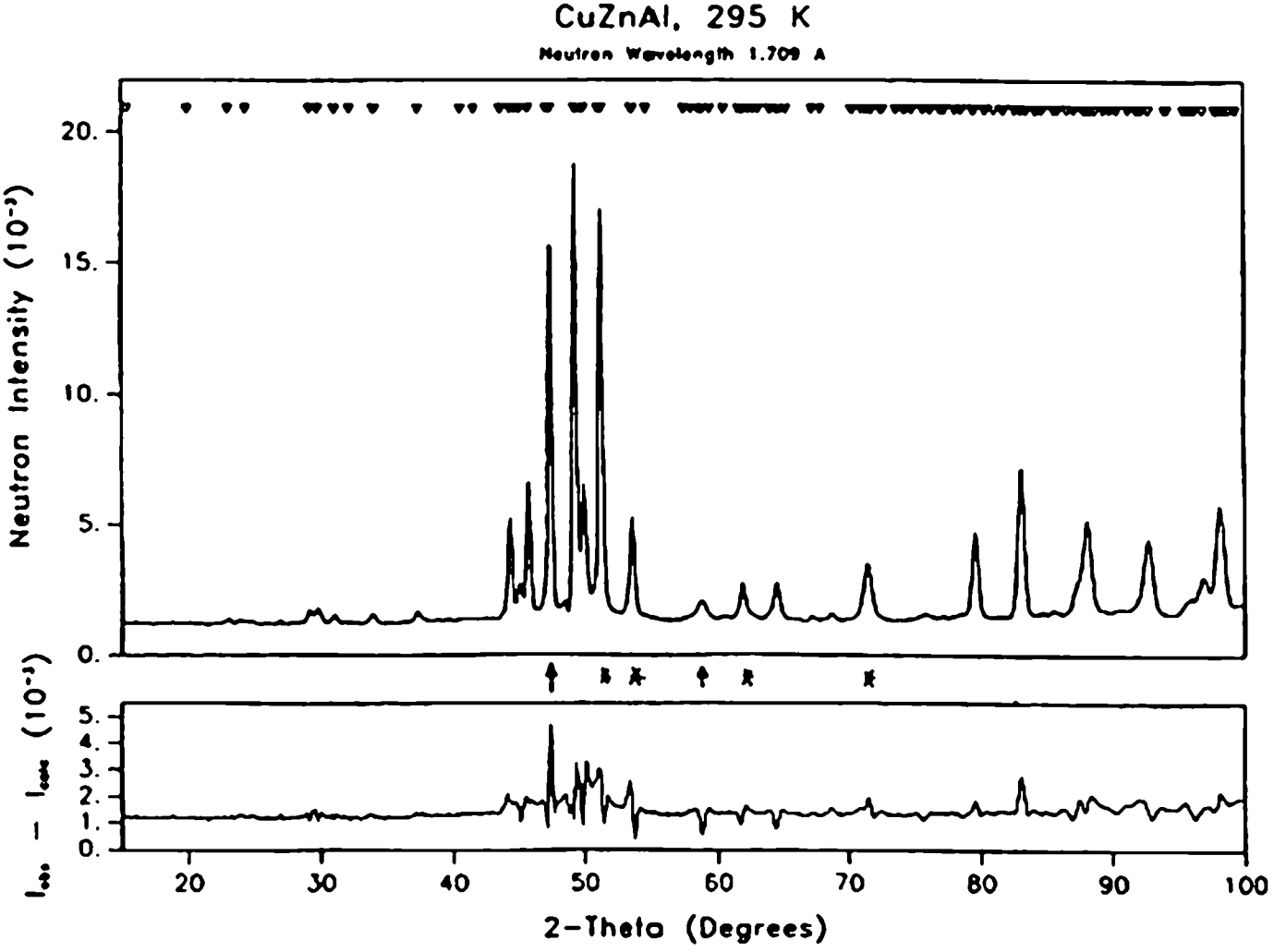

Fig. 2: Neutron diffraction intensity and difference observed minus calculated intensity. The measurements have been perfomed on the multidetector powder spectrometer DMC at the Laboratory of Neutron Scattering (ETH Zürich).

Stacking faults

A possible reason for the differences between model and powder measurement is the unperfect lattice. To study the influence of stacking faults on neutron diffraction peaks, computer calculations have been done. A computer program produces first a stacking sequence with a given number of faults and then calculates neutron intensity distributions along streaked reciprocal lattice rows. The result is shown in table 1. The peak positions of the reflection will be shifted from the regular positions. In addition, faulting leads to broadening and change in the integrated intensity of reflections. For some selected peaks measurements of the peak shifts and widths have been performed and the results were compared with computed values (see also table 1).

Mean dist. of faults / Fault type / Reflection		8192.0 a	48.0 a	24.0 a	48.0 b	24.0 b	observed values
(402)	width	0.006	0.056	0.079	0.056	0.079	0.091
strong	shift	0.000	-0.017	-0.033	0.017	0.033	0.025
(202)	width	0.009	0.060	0.083	0.059	0.083	0.089
strong	shift	0.000	0.018	0.036	-0.018	-0.036	-0.043
(002)	width	0.009	0.111	0.152	0.113	0.152	0.237
strong	shift	0.000	-0.001	-0.001	0.001	0.001	-0.001
(401)	width	0.007	0.032	0.045	0.032	0.044	0.078
medium	shift	0.000	0.010	0.020	-0.010	-0.021	-0.017
(201)	width	0.013	0.110	0.149	0.108	0.150	0.169
weak	shift	0.000	0.009	0.018	-0.010	-0.019	-0.030
(001)	width	0.008	0.081	0.111	0.080	0.111	0.076
weak	shift	0.000	-0.019	-0.038	0.019	0.039	0.037

Table 1: Calculated and observed peak shifts and widths for some selected peaks. For the calculations a cell with 8192 planes was used with random distributed stacking faults built in. The left column shows the values for a nearly perfect lattice. Note that the indices of the reflections correspond to the crystallographic unit cell. Shifts and widths are given in hkl-units too.

In the calculations two different fault types are used:

Type "a": △ △ ▽ △ △ ▽ △ ▽ △ △ ▽ △ △ ▽

Type "b": △ △ ▽ △ △ ▽ △ △ △ ▽ △ △ ▽ △

Kabra et al. (3) show, that 14 unique intrinsic stacking faults are possible in the 9R Structure. Keeping the separation of Cu and Al atoms on two different sublattices the number of possible stacking fault is the same in the 18R structure. To our mind,

stacking faults are predominantly of "b" type ("a" and "b" are called $I_{0,0}$ and $I_{2,1}$ in (3)). The model with faults of this type and with mean distance of 24 planes shows a good qualitative agreement. For a detailed quantitative analysis including other types of stacking faults more calculations and measurements are required.

Conclusions

The martensitic phase transition with memory-effect in Cu-Zn-Al is well known, however the driving force as well as the subsequent behaviour in the martensite (aging) are not clear. For a better understanding, acknowledge of the crystal structure, i. e. atomic distributions and coordinates in both phases, is highly desirable.
The present structure investigation show that conventional techniques fail because Cu-Zn-Al martensite is a strongly 'non-ideal' crystal. By taking into account stacking faults not only intensites change, but also positions of Bragg peaks are shifted. Therefore in a scattering experiment on a single crystal, an a priori distribution of faults (type, concentration) has to be given in order to perform proper scans in reciprocal space. On the other hand, in a powder experiment, all the information is contained in the measured intensities; however only integrated and with overlaps. Furthermore standard programs for profile analysis cannot be used.
Good results can only be obtained by combining the different methods, i.e.

(i) calculations on a 'real' crystal structure,
(ii) scattering experiments on a mono-domain martensitic crystal in order to check the model assumptions of (i),
(iii) analysis of powder diagrams with improved refinement programs.

Further work along these lines is in progress.

References

(1) D. Pandey and P. Krishna: in "Current Topics in Materials Science" (edited by E. Kaldis), 9, North-Holland, Amsterdam (1982) 415
(2) A. Dönni: Diplomarbeit, LNS-Report 136, Labor für Neutronenstreung ETH Zürich (1987) 48
(3) Kabra et al.: Acta metall. 36, (1988) 727